# FISSION OF RELATIVISTIC NUCLEI WITH ELECTROMAGNETIC EXCITATION*

Yasemin Kucuk

Department of Physics, Akdeniz University, Antalya, Turkey

Carlos A. Bertulani

Department of Physics and Astromomy, Texas A&M University-Commerce
Commerce, TX 75429, USA

In this work, we present a new approach to produce isotopic distribution of fission fragments in relativistic heavy-ion collisions. We take into account the collective excitation after the production of the primary fragments and explain simultaneously the production of fission yields as well as the heavy and light fragments.

## 1. Introduction

Isotopic distributions after peripheral collisions at relativistic energies have been studied over the years [1–5]. However, there is a long-standing problem in understanding the nuclide cross sections in these reactions. The experimental results could only be reproduced by systematic increasing the excitation energy by a factor of 2–3. Although doubling the excitation energies of the single-particle states provides a better agreement with fission data, it is not fully successful because it is not able to explain the cross section for the light- and intermediate-mass fragments. Therefore, we present a novel approach to compute isotopic distribution of fission fragments in relativistic heavy-ion collisions by using a combination of reaction models. We consider an additional energy that is generated by electromagnetic excitation of the primary fragments in the field of the reaction partners. We apply our model to the $^{238}$U+$^{208}$Pb at 1 GeV/nucleon.

---

## 2. Model

In this work, all relevant cross sections have been calculated within existing reaction formalisms, but with the additional inclusion of post-excitation and decay of the primary fragments. The peripheral collisions are typically fragmentation reactions. At impact parameters below the grazing impact parameter, one or several nucleons can be removed in the spontaneous interaction. This process is called abrasion and it has been theoretically studied in the framework of the microscopic and macroscopic approaches. Here, we use the Glauber model [6] to calculate the production cross section of primary fragments using Eq. (1)

$$
\sigma(Z_{\mathrm{F}}, N_{\mathrm{F}}) = \begin{pmatrix} Z_{\mathrm{P}} \\ Z_{\mathrm{F}} \end{pmatrix} \begin{pmatrix} N_{\mathrm{P}} \\ N_{\mathrm{F}} \end{pmatrix} \int \mathrm{d}^2 b \, [1 - P_p(b)]^{Z_{\mathrm{P}} - Z_{\mathrm{F}}}
$$
$$
\times P_p^{Z_{\mathrm{F}}}(b) \, [1 - P_n(b)]^{N_{\mathrm{P}} - N_{\mathrm{F}}} \, P_n^{N_{\mathrm{F}}}(b) , \tag{1}
$$

where $b$ is the impact parameter and $Z_{\mathrm{F}}$ protons (neutron also) can be removed from the $Z_{\mathrm{P}}$ initial protons of the projectile. Also, $P_p$ ($P_n$) are the probabilities for the survival of a single proton (and neutron) of the projectile and the factors containing $(1 - P)$ account for the removal probability of the other protons (neutrons). $P_p$ is the probability given by

$$
P_p(b) = \int \mathrm{d}z \, \mathrm{d}^2 s \rho_p^P(\boldsymbol{s}, z) \exp \left[ -\sigma_{pp} Z_{\mathrm{T}} \int \mathrm{d}^2 s \rho_p^{\mathrm{T}}(\boldsymbol{b} - \boldsymbol{s}, z) \right.
$$
$$
\left. - \, \sigma_{pn} N_{\mathrm{T}} \int \mathrm{d}^2 s \rho_n^{\mathrm{T}}(\boldsymbol{b} - \boldsymbol{s}, z) \right] , \tag{2}
$$

where $(Z_{\mathrm{T}}, N_{\mathrm{T}})$ is the charge and neutron number of the target, $\rho_p$ ($\rho_n$) is the proton (neutron) density of the projectile and target, which is normalized to unity. $\sigma_{np}$ and $\sigma_{pp}$ are the neutron–proton and proton–proton total cross sections, which have been taken from a fit to the experimental data. The neutron and proton single-particle densities have been generated by using the deformed Woods–Saxon model for the projectile nucleons. We have calculated the abrasion of projectile nucleons using the singe-particle states which have been generated in a deformed Woods–Saxon model [7] with a deformation parameter $\beta = 0.29$, radius $R_0 = 6.8$ fm, and diffuseness $a = 0.6$ fm. The depth of the potentials has been adjusted to produce the last occupied nucleon orbital with binding energy equal to the nucleon separation energy. The target density of $^{208}$Pb has been taken from electron scattering experiments [8].

Abrasion probabilities were calculated using Eq. (2) with radial and angular wave functions building up single-particle densities for each state. After the abrasion stage, the primary fragment excitation energy has been calculated from the particle–hole energies of the configuration relative to the

ground state. In this work, we use the post-excitation of primary fragments as a new technique to obtain isotopic distributions of the fission fragments. The excitation amplitude $\mathcal{A}_\alpha(z, b)$ of relativistic projectiles undergoing fission in-flight is obtained from the coupled-channels equation

$$i\hbar v \frac{\partial \mathcal{A}_\alpha(z, b)}{\partial z} = \sum_{\alpha'} \langle \alpha \left| \mathcal{M}_{(\text{E/N})\text{L}} \right| \alpha' \rangle \mathcal{A}_{\alpha'}(z, b) \, e^{-(E_{\alpha'} - E_\alpha)z/\hbar v} , \qquad (3)$$

where $b$ is the impact parameter, $v$ is the velocity, and $z$ is the projectile position along the beam direction. $\mathcal{M}_{\text{EL}}$ is the electromagnetic operator for electric dipole and quadrupole transitions. $\mathcal{M}_{\text{NL}}$ is corresponding the nuclear transition operator for the multipolarity $L$. In our calculations, we consider the excitation of the isovector giant dipole, isoscalar giant quadrupole, and isovector giant quadrupole resonances as well as the double giant dipole resonance. The main contribution to nuclear excitation comes from the excitation of the isoscalar giant quadrupole resonance. The matrix element for the transition $\alpha \longrightarrow \alpha'$ is given by [9]

$$\langle \alpha \left| \mathcal{M}_{N2m} \right| \alpha' \rangle = -\frac{\delta_2}{\sqrt{5}} \, \langle J_{\alpha'} M_{\alpha'} | Y_{2m} | J_\alpha M_\alpha \rangle \, Y_{2m}(\hat{\boldsymbol{r}}) \, \frac{\mathrm{d}U(r)}{\mathrm{d}r} , \qquad (4)$$

where $\delta_2$ is the deformation length, $U(r)$ is the scalar Lorentz-boosted nucleus–nucleus potential [10]. The optical potential in Eq. (4) is generated from the $t\rho\rho$ approximation [11] and a deformation parameter $\delta_2 = 0.438\,\text{fm}$ has been used. The excitation probabilities and then cross sections have been obtained from the solution of the coupled equations (3). The excitation of giant resonances by the nuclear and the Coulomb interactions provide large cross sections. We have used location at $E_{\text{IVGDR}} = 31.2A^{-1/3} + 20.6A^{-1/6}$ MeV for isovector giant dipole resonance and the double giant dipole resonance located at twice the IVGDR energy [11]. The isoscalar and isovector giant quadrupole resonance states are located at $E_{\text{ISGQR}} = 62A^{-1/3}$ MeV and $E_{\text{IVGQR}} = 130A^{-1/3}$ MeV, respectively [9, 11].

The cross sections for the projectile in the final state $|\alpha\rangle$ are obtained by an integration over impact parameters. We have solved the coupled equations (3) and calculated the probabilities of EM excitation of fragments on the outgoing part of their trajectories and weighted with the giant resonance energies. To take into account additional energy, we have added the fragment abrasion energy. In figure 1, we show the average excitation energies of protactinium (Pa) fragments due to abrasion. The additional EM energy is almost constant (13.3–13.7 MeV) for the Pa fragments. Similar results have been found for uranium [12], thorium, actinium, radium, and other heavy elements.
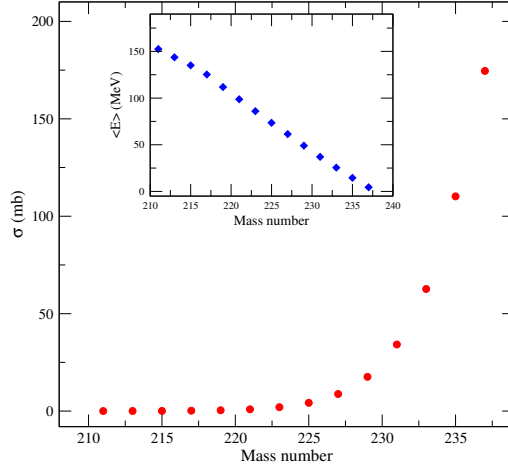
Fig. 1. Large frame: Cross sections for production of primary protactinium fragments due to projectile abrasion in the $^{238}$U+$^{208}$Pb reaction at 1 GeV/nucleon. Small frame: Average excitation energies of a few protactinium fragments due to abrasion.

After the excitation, the fragments will decay, mostly by the emission of light particles and $\gamma$-rays, but also into fission channels. At the ablation stage, light-charged particles, photon emission, and intermediate-mass fragments as well as fission products have been obtained by using the Ewing–Weisskopf model, using the ABLA07 code [13]. The separation energies have
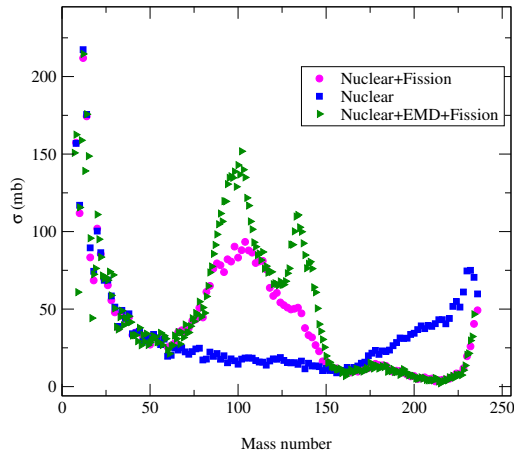


Fig. 2. (Color online) Mass distribution of projectile fragments produced in the $^{238}$U+$^{208}$Pb reaction at 1 GeV/nucleon. The blue diamonds correspond to the yields obtained with the abrasion–ablation model without fission contribution, while the violet circles include fission decays. The green arrows include the electromagnetic excitation leading to particle evaporation and fission products.

been taken from the 2016 atomic mass evaluation [14] and also emission barriers for charged particles has been calculated by using the Bass potential [15]. Fission yields have been calculated using the methodology which has been reported in Refs. [16, 17].

The cross sections for the mass distribution of each fragment have been calculated using the evaporation model after abrasion and electromagnetic (EM) excitation and shown in Fig. 2. In Fig. 3, we present the isotopic distribution of ruthenium fragments produced in the $^{238}$U+$^{208}$Pb reaction at 1 GeV/nucleon. The data have been taken from Ref. [18]. We have obtained very good agreement with the data as shown in the figure.
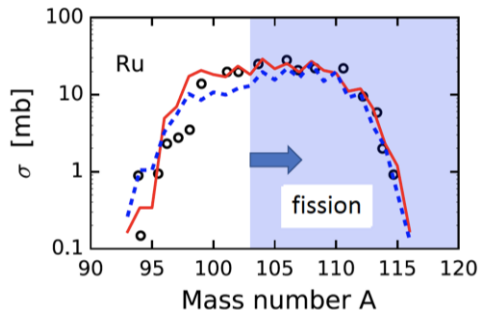


Fig. 3. (Color online) Isotopic distribution of ruthenium fragments produced in the $^{238}$U+$^{208}$Pb reaction at 1 GeV/nucleon. The data (open circles) have been taken from Ref. [18]. The solid (dashed) lines correspond to fragmentation calculations with (without) the inclusion of final-state electromagnetic excitation of abraded fragments. The arrows point to the region (shaded area) of increasing contribution of fragments decaying by fission.

## 3. Conclusion

We have presented a new approach to account for the excitation energy of the fragments. It has been a long-standing problem that the energy deposited in the nucleus is not enough to explain the fragment yields in the fragmentation of relativistic nuclei. To overcome this problem, the excitation energy has been multiplied so far by a factor of 2–3 in the calculations instead of using the exact excitation energy obtained in the framework of the original abrasion–ablation model. By using this method, reasonable agreement has been obtained with the experimental data. In this paper, we have shown that this multiplication factor is not necessary for the peripheral collisions involving heavy nuclear targets and the additional energy is generated by electromagnetic excitation in the field of the heavy target. We have shown the all results and discussions in detail in Ref. [12].

## REFERENCES

[1] K.-H. Schmidt, B. Jurado, *Rep. Prog. Phys.* **81**, 106301 (2018).

[2] K.-H. Schmidt *et al.*, *Nucl. Phys. A* **665**, 221 (2000).

[3] T. Aumann *et al.*, *Z. Physik A — Hadrons and Nuclei* **352**, 163 (1995).

[4] P. Armbruster *et al.*, *Z. Physik A — Hadrons and Nuclei* **355**, 191 (1996).

[5] J. Benlliure *et al.*, *Nucl. Phys. A* **628**, 458 (1998).

[6] J. Hüfner, K. Schäfer, B. Schürmann, *Phys. Rev. C* **12**, 1888 (1975).

[7] A. Kruppa, Z. Papp, *Comput. Phys. Commun.* **36**, 59 (1985).

[8] H.D. Vries, C.D. Jager, C.D. Vries, *At. Data Nucl. Data Tables* **36**, 495 (1987).

[9] G. Satchler, *Nucl. Phys. A* **472**, 215 (1987).

[10] C.A. Bertulani, *Phys. Rev. Lett.* **94**, 072701 (2005).

[11] C.A. Bertulani, V. Ponomarev, *Phys. Rep.* **321**, 139 (1999).

[12] C.A. Bertulani, Y. Kucuk, R. Lozeva, *Phys. Rev. Lett.* **124**, 132301 (2020).

[13] A. Kelic, M.V. Ricciardi, K.-H. Schmidt, arXiv:0906.4193 [nucl-th].

[14] W.J. Huang *et al.*, *Chinese Phys. C* **41**, 30002 (2017).

[15] R. Bass, «Nuclear Reactions with Heavy Ions, Texts and Monographs in Physics», *Springer Verlag*, Heidelberg 1980.

[16] B. Jurado, K.-H. Schmidt, J. Benlliure, *Phys. Lett. B* **553**, 186 (2003).

[17] B. Jurado *et al.*, *Nucl. Phys. A* **747**, 14 (2005).

[18] T. Enqvist *et al.*, *Nucl. Phys. A* **658**, 47 (1999).